Modeling the Effect of Surface Roughness on the Performance of Line Tunnel FETs

Saurabh Sant and Andreas Schenk
Integrated Systems Laboratory,
ETH Zurich,
Zurich, Switzerland
sasant@iis.ee.ethz.ch

***Abstract*— Surface roughness causes random shifts in the lowest sub-band level around its ideal position. This gives rise to tail states of an otherwise step-like DOS of the 2D electron gas in the channel. These tail states cause a gradual onset of tunneling in a TFET with vertical tunnel paths and degrade the sub-threshold swing. The impact of roughness of the semiconductor/oxide interface on the transfer characteristics is analyzed in this paper. Quantum-mechanical calculations are performed on a (pseudo)-one-dimensional TFET to obtain the drain current in the presence of randomly shifted sub-band levels. It is found that, the larger the roughness amplitude, the stronger the degradation of the sub-threshold swing.**

Keywords*— *Surface roughness, Tunnel FETs, Line tunneling.

I. Introduction

To minimize the frequency of charging batteries, it is necessary to reduce the energy footprint of integrated circuits used in mobile communication equipment. Supply voltage scaling is one way of reducing energy consumption in integrated circuits. However, due to the physical limit on the mechanism of operation of Metal Oxide Semiconductor Field Effect Transistors (MOSFETs), the supply voltage of MOSFET based integrated circuits cannot be further scaled at this stage. Therefore, alternative energy-efficient solid-state electronic switches are sought after to replace MOSFETs. The Tunnel Field Effect Transistor (TFET) is a switch which works on the principle of band-to-band tunneling (BTBT) in semiconductors. It offers the possibility of scaling down the supply voltage [1].

In a TFET, BTBT either takes place parallel to the gate (often referred to as point tunneling), perpendicular to the gate (often called line tunneling), or inclined. In a vertical TFET, called Line TFET (LTFET) in the following, vertical tunneling prevails. With the special device geometry shown in Fig. 1(a) point tunneling can be completely suppressed. Line tunneling takes place between two-dimensional electronic states in the triangular well at the oxide-semiconductor interface and the three-dimensional hole states in the bulk region. A sharp step-like onset of BTBT is a peculiar characteristic of the 2D-3D DOS matching. This sharp onset of BTBT results in a small sub-threshold swing (SS). Scaling of the gate area can scale up the on-state current in a LTFET. However, field-induced quantum confinement in the channel degrades the on-current [2,3]. Additionally, the rough oxide-semiconductor interface results in band tail states [4] which cause a more gradual onset of line tunneling and thereby degrades the SS.

Funding from the European Community's Seventh Frame-Work Program under Grant Agreement No. 619509 (Project E²SWITCH) is acknowledged.

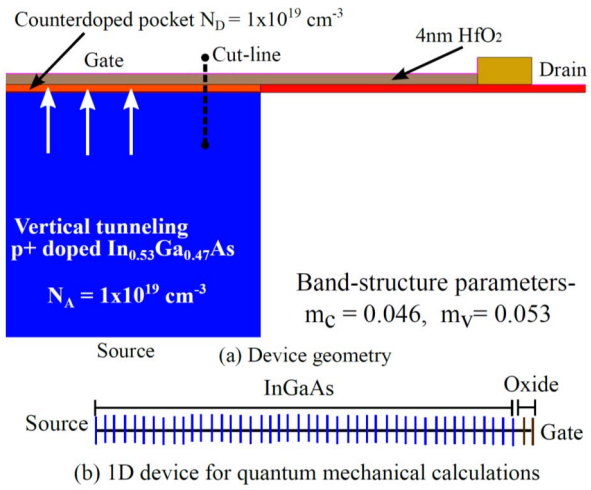

Figure 1: (a) InGaAs LTFET with counter-doped pocket. The special geometry favors vertical ("line") tunneling and is used to analyze the impact of channel quantization and surface roughness. (c) (Pseudo-) one-dimensional TFET used for quantum-mechanical calculations.

In this work, the impact of surface roughness on the steepness of transfer characteristics of LTFETs is analyzed. Quantum-mechanical calculations are performed to obtain the tunnel current for sub-band edges at different energies adjacent to the energy of the first sub-band. The drain current for a LTFET with surface roughness is calculated by an ensemble average of these tunnel currents. The variation of the influence of surface roughness with source and channel doping is analyzed. Finally, the drain current resulting from the quantum-mechanical calculations is compared with that obtained from the semi-classical model from [3].

II. Simulation Set-up

The special geometry of a LTFET which suppresses point tunneling is shown in Fig. 1(a). The wide gate overlapped on the source region provides a large area for vertical tunneling. The thin long undercut region between the source edge and drain ensures low off-state leakage. A 5 nm thick counter-

doped pocket is introduced under the gate to advance the onset of the device. A two-dimensional quantum transport simulation of such a large device is computationally not feasible. Therefore, a cut-line normal to the interface was used for one-dimensional quantum-mechanical calculations. This uni-dimensional device is schematically shown in Fig. 1(b).

A. Quantum-mechanical Calculation of the Tunnel Current

The one-dimensional device in Fig. 1(b) is simulated using a self-consistent 1D k·p-Poisson solver available in the S-Band package [5]. For each gate bias, the energy levels and the quantized electron wave functions of the first sub-band are obtained from the solver. The Numerov method is used to calculate the valence band (VB) wave functions in the bulk region for all energies $E^{\perp}$ of the tunnel window. The tunnel probability is calculated for each $E^{\perp}$ using Fermi's golden rule. The total drain current per unit gate area is then calculated in the Landauer formalism. The entire procedure is described below.

The triangular potential well in the channel results in the quantization of the conduction band (CB) states. These states are obtained by solving the following envelope equation numerically using a 1D k·p-Poisson solver available in S-Band [5]:

$$\left(-\frac{\hbar^2}{2m_c}\frac{d^2}{dx^2}+U(z)\right)\chi_{c,n}(z)=E_n\,\chi_{c,n}(z). \qquad (1)$$

For Eq. (1) it is assumed that the device is homogeneous in the xy-plane. Hence, the x- and y-dependent components of the envelope function are given by plane waves. This adds an additional energy term to the total energy. The total energy thus becomes $E_{n,\perp}=E_n+E^{\perp}$.

Since VB states are not quantized, an envelope function exists for each available value of $E^{\perp}$. The envelope functions for the VB states are obtained solving the following equation by the Numerov algorithm:

$$\left(-\frac{\hbar^2}{2m_v}\frac{d^2}{dx^2}+(U(z)-E-E')\right)\chi_v(z,E')=0. \qquad (2)$$

Hard-wall boundary conditions at the oxide-semiconductor interface ($\chi_v(z=0,E^{\perp})=0$) are used as boundary condition for the wave function as required for the Numerov algorithm.

The envelope functions for the CB and VB states obtained by the above method are exact solutions of the Schrödinger envelope equation. The inter-band matrix element as a function of $E^{\perp}$ can be obtained by treating the field-dependent inter-band coupling term as perturbation,

$$M_{n,v}(E_{n,\perp},E')=\int_0^{\infty}\chi_{c,n}(x)\,H'(x)\,\chi_v(x,E')dx, \qquad (3)$$

$$\text{where } H'(x)=\frac{\hbar\cdot P}{m_0\cdot E_g}\nabla U(x).$$

Here, P is the momentum matrix element and E_g is the band gap. The tunnel probability can then be calculated using Fermi's golden rule,

$$T(E')=\frac{2\pi}{\hbar}\int_{E_n}^{E_{max}}\left|M_{n,v}(E_{n,\perp},E')\right|^2\delta(E_{n,\perp}-E')dE_{n,\perp}. \qquad (4)$$

Note that although E_n is discrete, $E_{n,\perp}$ is continuous as it involves the transverse energies. The above integral gives a Heaviside function on integration, which implies that $E'>E_n$ for tunneling to take place. The total electron current can be calculated by integrating the tunnel probability over all available transverse energies,

$$J_T=\int_0^{E_{max}}T(E'^{\perp})\rho(E'^{\perp})dE'^{\perp}. \qquad (5)$$

The current density obtained by this approach is in units of A/m^2. It can be multiplied by the gate area to obtain the drain current. In this way, the drain current is calculated per unit area for the given sub-band energy.

B. Introducing the Effect of Surface Roughness in the Calculation

The oxide-semiconductor interface (assumed to be in the xy-plane) is not atomistically smooth. Its roughness causes random shifts of the (assumed infinitely high) potential wall of the triangular well along the z-axis. This results in random shifts of the first sub-band level around its mean energy as

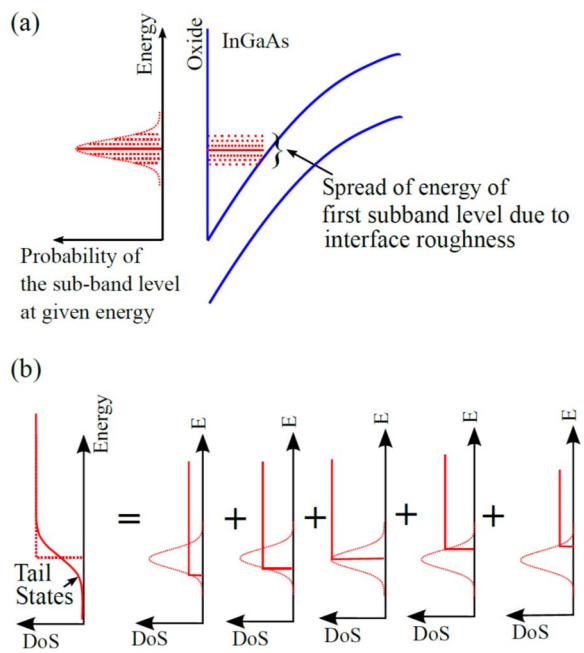

Figure 2: (a) Schematic showing the Gaussian spread of the energy of the first sub-band level. (b) Sketch of the weighted average of the DOS of all the randomly shifted first sub-band levels resulting in an error-function like DOS with tail states below the mean sub-band level.

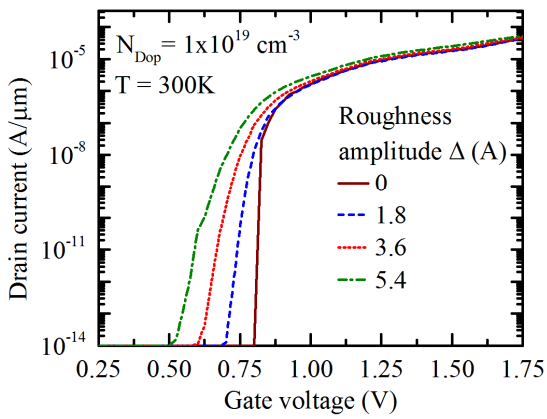

Figure 3: Comparison of transfer characteristics of the uni-dimensional LTFET for different values of the roughness amplitude.

shown in Fig. 2(a). This means that the value of the first sub-band energy level is different at different locations in the xy-plane. If the sub-system at each location in the xy-plane acts as an independent 2D sub-system, the DOS of the quantized electronic states in the sub-system is step-like. The average DOS of the total system is obtained by taking the weighted average of the DOS of each of such localized sub-systems at each location in the xy-plane. The weights are the probability of existence of a sub-band level at a given energy. For a rough interface with Gaussian correlation, the spread of the sub-band levels is a Gaussian with the center at the mean energy of the first sub-band as shown in Fig. 2(a). Averaging of the DOS as described above with a Gaussian as a weighing function results in the average DOS with the shape of an error function as depicted schematically in Fig. 2(b). The aggregate effect of this random shift of the sub-band level is the formation of band tail states below the mean energy.

The quantum-mechanical treatment of a 2D electronic system in the presence of an arbitrary random potential in 2D by Quang and Tung [6] yields an error-function-like DOS which is in agreement with our argument described above. The standard deviation (η) appearing in the Gaussian distribution and the error function is calculated in [8] by inserting Ando's roughness potential [7] as an arbitrary random potential. It is given by,

$$\eta = F_{\text{eff}}\,\Delta\,, \qquad (6)$$

where η is the characteristic energy, F_{eff} is the effective electric field given by $F_{\text{eff}} = \frac{\int_0^T dz\, F(z)\cdot n(z)}{\int_0^T dz\, n(z)}$, and Δ is the roughness amplitude.

Assuming that the tunnel rate can be independently calculated for each localized sub-system, the total tunnel current in the presence of surface roughness is given by

$$I_{\text{DS}} = \frac{A}{\eta\sqrt{\pi}} \int_{-\infty}^{E_{\max}} J_{\text{T}}(E)\, \exp\left(-\frac{(E-E_0)^2}{2\eta^2}\right)\, dE. \qquad (7)$$

Here, $J_{\text{T}}(E)$ is the drain current calculated by the quantum-mechanical treatment described in sub-section II-A (see Eqs. (1) - (5)) for a system with the sub-band lying at energy E. In this way, the *total* drain current is calculated by taking the ensemble average of the drain currents arising from the spread out levels of the first sub-band at each of the energies E ($-\infty < E < E_{max}$) around the mean sub-band level (E_0).

III. Simulation Results and Discussion

The drain current in the presence of broadened sub-band energies due to surface roughness was calculated using the above described procedure. A roughness amplitude Δ of 1.8 Å and a correlation length L of 1.9 nm was experimentally extracted for a InAs/GaSb hetero-junction by Feenstra *et al.* [9] Also, roughness amplitudes ranging between 5 Å and 11 Å have been reported for thin $In_{0.75}Ga_{0.25}As$ pHEMT structures [10]. Taking these values as guidelines, the quantum-mechanical calculations were performed with $\Delta = 1.8$ Å, 3.6 Å, and 5.4 Å. The simulation results are presented in Fig. 3. As observed in the figure, an increasing roughness amplitude degrades the sub-threshold swing, as one would

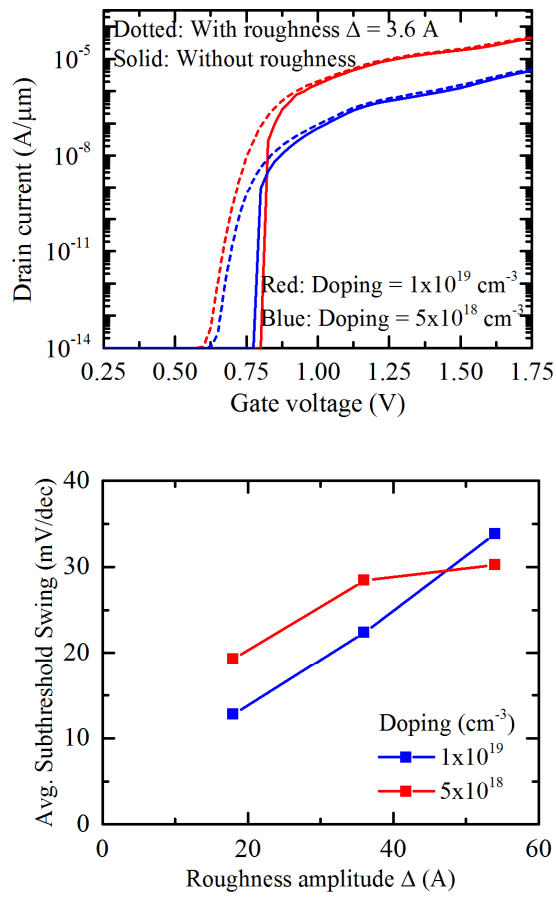

Figure 4: Comparison of (a) transfer characteristics and (b) sub-threshold swing of the LTFET with and without considering surface roughness for two different values of the bulk doping.

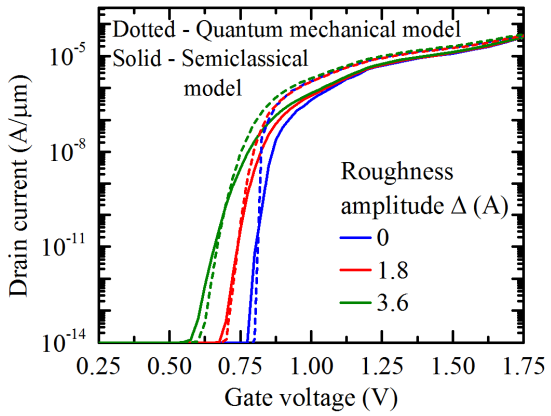

Figure 3: Comparison of transfer characteristics of the 1D LTFET calculated quantum-mechanically and by the semi-classical model for different values of the roughness amplitude.

expect. The sub-threshold swing averaged over four orders of magnitude of the drain current is plotted vs. roughness amplitude in Fig. 4(b) (blue line). The plot confirms that the steepness of the *IV*-plots at the onset degrades with increasing Δ.

The effect of the source doping level on the *IV*-plots with and without roughness was studied by calculating the transfer characteristics for two doping concentrations, 5×10^{18} cm^{-3} and 1×10^{19} cm^{-3}. The *IV*-curves are compared in Fig. 4(a). The average sub-threshold swing of the LTFET is plotted in Fig. 4(b) vs. roughness amplitude for the two doping values. The lower the doping, the smaller F_{eff} and the characteristic tail energy η. Hence, the reduction of doping is expected to result in a lowering of the sub-threshold swing. On the other hand, a smaller doping concentration increases the tunnel length which in turn degrades the sub-threshold swing. A degradation of the swing due to the reduced doping is observed for smaller Δ . For $\Delta = 5.4$ Å, the effect of a smaller η due to lower doping becomes dominant and the subthreshold swing is improved with decreasing doping concentration.

A. Comparison with Semi-classical Model

A semi-classical TCAD model was presented in [8] to account for the formation of band tails due to interface roughness and their impact on line tunneling. Here, this model is employed on the uni-dimensional LTFET for comparison. The band diagrams extracted from the k·p-Poisson solver at each bias point are processed to obtain the active tunnel paths. The semi-classical model is then used on these tunnel paths to calculate the tunnel current. In Fig. 5, the drain current obtained from the quantum-mechanical calculations is compared with the semi-classical drain current. The good agreement confirms the validity of the semi-classical TCAD model.

It must be noted that the above treatment is only applicable for vertical (line) tunneling. Furthermore, various non-idealities such as bulk band tails, interface and bulk traps, etc. affect the TFET performance in addition to interface roughness. It is observed that, among all the non-idealities, traps have the strongest impact [11]. However, the detrimental effect of traps is going to fade out with improving technology. If that happens, interface roughness may become an important non-ideality that degrades the sub-threshold swing.

IV. Conclusion

In summary, the impact of a rough semiconductor/oxide interface is assessed by quantum-mechanical calculations of a uni-dimensional LTFET. The simulations show that surface roughness degrades the sub-threshold swing and results in a gradual turn-on of the device instead of a sharp, step-like onset. The larger the roughness amplitude Δ, the more severe the degradation of the sub-threshold swing. Also, for larger values of Δ, reducing the source doping reduces the degradation of the swing. It must be noted, that the above results only apply to vertical (line) tunneling.

References

[1] A. M. Ionescu, H. Riel,"Tunnel field-effect transistors as energy-efficient electronic switches, Nature vol. 479, pp. 329–337, 2011.

[2] S. Goodnick, R. Gann, D. Ferry, C. Wilmsen, and O. Krivanek, "Surface roughness induced scattering and band tailing, Surface Science vol. 113, pp. 233–238, 1982.

[3] W. G. Vandenberghe, B. Soree, W. Magnus, G. Groeseneken, A. Verhulst, and M. V. Fischetti, "Field induced quantum confinement in indirect semiconductors: Quantum mechanical and modified semiclassical model, SISPAD'11, pp. 271–274 (2011).

[4] S. Sant, A. Schenk, K. Moselund, and H. Riel, "Impact of Trapassisted Tunneling and Channel Quantization on InAs/Si Hetero Tunnel FETs", 74th IEEE Device Research Conference, pp. 67–68, 2016.

[5] Synopsys Inc., Device Monte Carlo User Guide, V-2015.06.

[6] D. Quang and N. Tung, "A Semiclassical Approach to the Electron Gas in Two-Dimensional Semiconductor Structures, phys. Stat. sol. (b), vol. 207, pp. 111–123, 1998.

[7] T. Ando, "Screening effect and quantum transport in Silicon inversion layer in strong magnetic fields", J. Phys. Soc. Japan, vol. 43, pp. 1616–1626, 1977.

[8] S. Sant and A. Schenk, "Modeling the Effect of Interface Roughness on the Performance of Tunnel FETs", IEEE Electron Device Lett., vol. 38, no. 2, pp. 258–261, 2017.

[9] R. M. Feenstra, D. A. Collins, D. Z.-Y. Ting, M. W. Wang, and T. C. McGill, "Interface roughness and asymmetry in InAs/GaSb superlattices studied by scanning tunneling microscopy, Phys. Rev. Lett. vol. 72, pp. 2749–2752, 1994.

[10] M. Naidenkova, M. S. Goorsky, R. Sandhu, R. Hsing, M. Wojtowicz, T. P. Chin, T. R. Block, and D. C. Streit, "Interfacial roughness and carrier scattering due to misfit dislocations in $In_{0.52}Al_{0.48}As/In_{0.75}Ga_{0.25}As/InP$ structures", J. Vac. Sci. Technol. B, vol. 20, no. 3, pp. 1205–1208.

[11] A. Schenk, S. Sant, K. Moselund, and H. Riel, "III-V-Based Hetero Tunnel FETs: A Simulation Study Focussed on Non-ideality Effects", Proc. ULIS-EUROSOI, pp. 9–12, 2016